Applied Physics Letters

Residual stress effect governing electromigration-based free-standing metallic micro/nanowire growth behavior

Cite as: Appl. Phys. Lett. **116**, 024102 (2020); https://doi.org/10.1063/1.5131710
Submitted: 15 October 2019 . Accepted: 02 January 2020 . Published Online: 16 January 2020

Yasuhiro Kimura, and Yang Ju

ARTICLES YOU MAY BE INTERESTED IN

Super-resolution photoluminescence lifetime and intensity mapping of interacting CdSe/CdS quantum dots
Applied Physics Letters **116**, 021103 (2020); https://doi.org/10.1063/1.5132563

Collective excitations in 2D atomic layers: Recent perspectives
Applied Physics Letters **116**, 020501 (2020); https://doi.org/10.1063/1.5135301

Interplay between emission wavelength and s-p splitting in MOCVD-grown InGaAs/GaAs quantum dots emitting above 1.3 μm
Applied Physics Letters **116**, 023102 (2020); https://doi.org/10.1063/1.5124812

Lock-in Amplifiers up to 600 MHz

© 2020 Author(s).

Residual stress effect governing electromigration-based free-standing metallic micro/nanowire growth behavior

Cite as: Appl. Phys. Lett. **116**, 024102 (2020); doi: 10.1063/1.5131710
Submitted: 15 October 2019 · Accepted: 2 January 2020 ·
Published Online: 16 January 2020

View Online

Export Citation

CrossMark

Yasuhiro Kimura[1,a] and Yang Ju[2]

AFFILIATIONS

[1]Department of Finemechanics, Graduate School of Engineering, Tohoku University, Aoba 6-6-01, Aramaki, Aoba-ku, Sendai 980-8579, Japan

[2]Department of Micro-Nano Mechanical Science and Engineering, Nagoya University, Furo-cho, Chikusa-ku, Nagoya 464-8603, Japan

[a]**Present address**: Department of Micro-Nano Mechanical Science and Engineering, Nagoya University, Furo-cho, Chikusa-ku, Nagoya 464-8603, Japan. **Author to whom correspondence should be addressed:** yasuhiro.kimura@mae.nagoya-u.ac.jp

ABSTRACT

In this study, the effect of residual stress in a film on the growth behavior of a free-standing metallic micro/nanowire due to electromigration (EM) is examined. The growth of a wire is accompanied by atomic diffusion, accumulation of atoms, and release of compressive EM-induced localized hydrostatic stress due to the accumulation of atoms. Hence, the growth of the wire dominantly depends on the EM-induced localized stress caused by the accumulation of atoms. Because rigid passivation generates a strong localized stress field in the metallic interconnect, with greater accumulation of atoms, the EM-induced localized stress state for wire growth is influenced by passivation conditions, including the thickness and residual stress associated with passivation. Two samples with different passivation thicknesses, resulting in different levels of residual stress, were used to elucidate the influence of passivation conditions on the growth performance of Al microwires. The growth rate was experimentally measured. An x-ray diffraction system was used to obtain the value of residual stress in passivation, demonstrating that a higher absolute value of compressive residual stress results in a lower growth rate. In contrast, a lower absolute value increases the growth rate of the wire and can decrease the delamination risk of the topmost passivation, deposited by sputtering. Contrarily, a passivation that is too thin, resulting in a lower absolute value of compressive stress, increases the risk of passivation crack due to the accumulation of atoms by EM. A suitable passivation thickness for a desired wire growth must be determined based on this finding.

Published under license by AIP Publishing. https://doi.org/10.1063/1.5131710

High-density electron flow in a metal causes atomic diffusion, referred to as electromigration (EM). In modern electronics, miniaturization results in narrow interconnects that increase the current density, increasing the risk of deterioration in an interconnect due to EM. EM deforms the interconnect as atoms are depleted and accumulated, causing voids and hillocks, respectively. The formation of a hillock is due to the fracture of the passivation film, which covers the metallic interconnect to provide protection from external damage and corrosion, by the EM-induced accumulation of atoms. This EM-induced accumulation corresponds to an increase in the absolute value of hydrostatic stress at a localized region in a metallic interconnect under passivation,[1–3] and the excess EM-induced localized hydrostatic stress decreases the reliability of integrated circuits with passivation fracture. Contrary to the many studies regarding the mechanics of suppressing EM-induced localized stress to increase the reliability of electronics, this study addresses the promising growth technique of metallic micro/nanowires (hereafter called the EM technique) through the EM-induced localized hydrostatic stress: recent works have attempted to use EM as a structuring tool to grow nanowires[4] and to form nanoscale small gaps and constrictions for molecular electronics.[5–8]

Hillocks, with a tiny cross-sectional area, grow as micro/nanowire, which is a one-dimensional (1D) micro/nano-scale structure. To date, in a metallic micro/nanostructure, a focus has been placed on 1D nanowires (also called whiskers) composed of Sn to clarify its growth mechanism, as Sn-based whiskers are often observed in integrated circuits with Pb-free solder composed of Sn. For Al, the self-growth mechanism and effective spontaneous growth technique for high-quality Al micro/nanowires have not

Published under license by AIP Publishing

yet been established owing to a lack of research, and so many research studies have been in progress,[9–14] although Al has been shown to be a promising material for application to plasmonic devices.[15–20] The EM technique is an expected growth technique for free-standing metallic micro/nanowires, in which an Al micro/nanowire would be formed with a high aspect ratio and a desired cross-sectional shape at an intended location.[21,22] However, the development of the EM technique is in its early stages, and progress is being made toward its establishment as a sophisticated growth technique for Al micro/nanowires. Thus, a firm scientific foundation still needs to be developed.

As reported in previous studies,[23–25] the growth of metallic micro/nanowires in the EM technique is accompanied by atomic diffusion, accumulation of atoms, and release of localized compressive hydrostatic stress due to the accumulation of atoms. The EM-induced localized higher compressive hydrostatic stress drives atoms out of a hole in the structure, i.e., atoms are discharged by the pressure difference due to the accumulation of atoms and atmospheric pressure. Discharged atoms form a metallic micro/nanowire, in which the size of the cross section of the wire depends on the hole size. Two key components in the EM technique exist: the artificial hole through which atoms are discharged and the passivation that allows localized stress to increase because of the accumulation of atoms by confining the deformation of interconnects. Past studies have elucidated the role of the artificial hole in the behavior of wire growth.[24,25] The size of the hole significantly impacts the performance of wire growth because the hole size can affect the loss of discharging atoms through the hole.[25] On the other hand, the passivation effect, also one of the key components, has not been yet delineated. In practice, even if the same values of the input current were used, the different passivation thicknesses, which cover the metallic interconnects, would lead to difficulty in the repeatability of wire growth.

This work aims to reveal the function of passivation thickness on the growth of a micro/nanowire and propose a design strategy to facilitate this wire growth through the EM technique. Because the passivation thickness influences the residual stress in a film, the relationship between the passivation thickness and wire growth behavior is discussed by experimentally measuring the residual stress in a film. Part of this study was preliminarily presented at a local conference in Japan.[26]

Figure 1 shows FE-SEM images and schematics of a sample structure with a bow-tie pattern, covered with TiN passivation for wire growth. In this study, an Al microwire was grown by the EM technique as an example of metallic micro/nanowire growth. The process for making the sample structure is based on those in previous studies.[23–25] The bow-tie Al interconnect is embedded into an Si wafer. The structure is composed of a 280-μm-thick Si wafer, 300-nm-thick SiO_2, Ti, and TiN underlayers, a 600-nm-thick Al interconnect, and TiN passivation: the thickness of TiN passivation will be described later. A focused ion beam introduced a hole in the TiN passivation with the hole side length D of 1.5 and 2.0 μm, through which Al atoms are extruded, resulting in the growth of the Al microwire.

Thicker rigid passivation confines the deformation of the interconnect at the localized region where the atoms are accumulated, and then the compressive EM-induced localized hydrostatic stress rises at this localized region. A thicker passivation can allow the accumulation of more atoms for wire growth: however, a passivation that is too thick

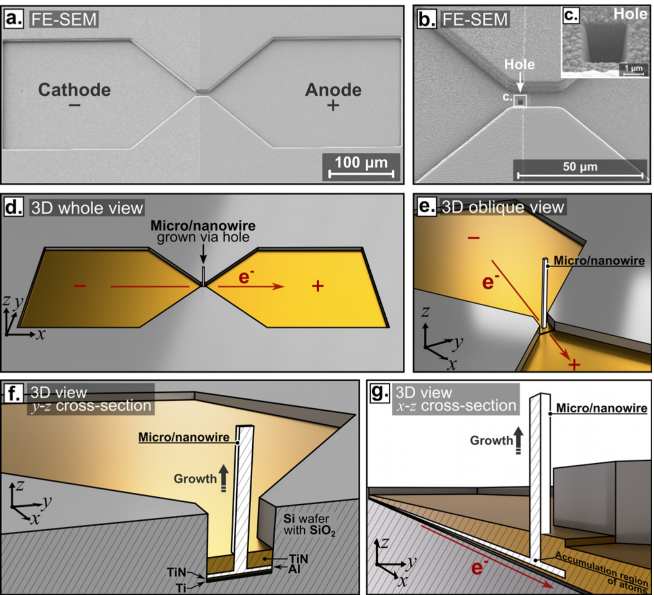

FIG. 1. Bow-tie sample structure composed of a 280-μm-thick Si wafer, 300-nm-thick SiO_2, Ti, and TiN underlayers, a 600-nm-thick Al interconnect, and 2.6- or 3.5-μm-thick TiN passivation: FE-SEM images of the (a) whole view, (b) magnified view around a hole, and (c) magnified view of a hole; and three-dimensional (3D) schematics of the (d) whole view, (e) oblique view, (f) *y-z* cross section (transverse plane), and (g) *x-z* cross section (longitudinal plane) around a wire. Hatching denotes the cross-sectional surface.

would be delaminated after immediate deposition as adhesive failure by own excessive compressive biaxial stress. The delamination of TiN passivation was empirically observed in the case where $H_{TiN} \geq 4.0\,\mu$m. Conversely, with the use of a thinner passivation, the accumulation of atoms would fracture the passivation easily, deforming the interconnect after the rupture of the passivation. Figure 2 shows the failure and favorable results of wire growth with thinner and thicker passivations of 2.0 and 2.6 μm, respectively. Based on the results shown in Fig. 2, the thickness of the passivation must be sufficient to facilitate wire growth; thus, this study adopts a passivation thickness of greater than or equal to 2.6 μm and less than 4.0 μm.

Two samples with different TiN passivation thicknesses H_{TiN} of 2.6 and 3.5 μm were used to investigate the effect of the passivation thickness on wire growth in the EM technique. To examine the influence of the passivation thickness on wire growth in terms of EM-induced localized stress, wire growth and the measurement of the residual stress in a film were carried out. The wire growth was conducted by stressing the electrical current under a fixed substrate temperature T_s of 773 K. The residual stress in the TiN passivation of the topmost layer was experimentally measured as biaxial stress using an x-ray diffraction (XRD) system (Bruker-AXS D8 Advance diffractometer, Cu-Kα, wavelength of 0.15406 nm) with a 2D detector (VÅNTEC-500). The Young's modulus of 424 GPa and Poisson's ratio of 0.200 were used for the calculation. The residual stress in the Al interconnect through which atoms are migrated owing to EM needs to be measured instead of the TiN passivation residual stress; however, it is difficult to measure the residual stress in the Al interconnect because it is covered with the TiN passivation. However, the residual stress of

Published under license by AIP Publishing

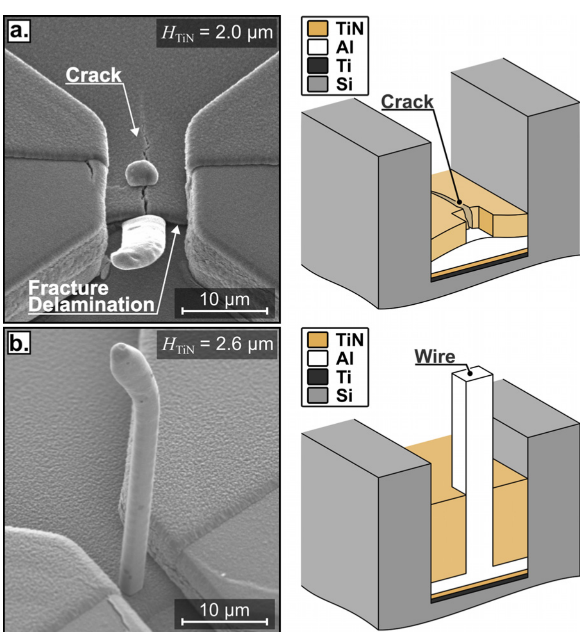

FIG. 2. FE-SEM images of the experimentally failure and favorable results of a wire growth with illustrations of the sample structure around a hole. (a) Failure and (b) favorable growth in the case of passivation thickness $H_{TiN} = 2.0$ and 2.6 μm. The passivation thickness required for wire growth was determined based on the experimental results.

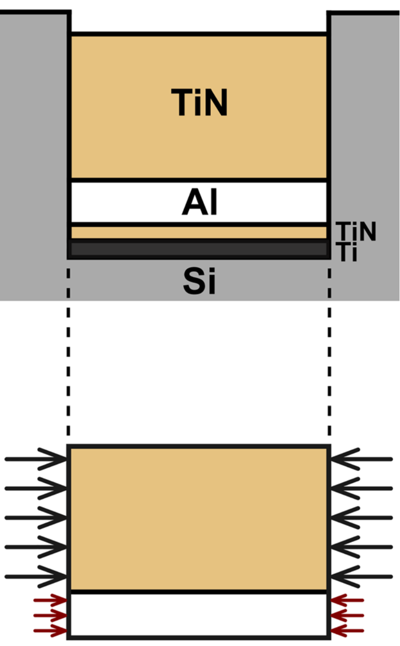

FIG. 3. Schematic of the *y-z* cross section (transverse plane) of the sample structure in the case of compressive biaxial stresses in the films. The stress state of TiN reflects the stress state of Al based on Eq. (1).

the TiN passivation would reflect the stress state of the entire area of the Al interconnect through the interface. For example, the Al has compressive residual stress when the TiN has compressive residual stress, based on Eq. (1) and as shown in Fig. 3,

$$(\sigma_{\mathrm{Al}})_{\mathrm{res}} = \frac{E_{\mathrm{Al}}}{E_{\mathrm{TiN}}}\frac{1-\nu_{\mathrm{TiN}}}{1-\nu_{\mathrm{Al}}}(\sigma_{\mathrm{TiN}})_{\mathrm{res}}, \tag{1}$$

where E is the Young's modulus and ν is Poisson's ratio. Equation (1) expresses the residual stress state of the Al interconnect and is always established based on the following assumptions: (I) the plane stress is considered because the thicknesses of the Al interconnect and TiN passivation are very thin compared with that of the Si wafer; (II) the strains of TiN and Al at the interface are the same because TiN and Al are tightly connected at the interface; and (III) the bending of the film is not considered because the value of the flexural rigidity of the TiN passivation is much greater than that of the Al interconnect. Because the residual stress in Al is proportional to that in TiN based on Eq. (1), the measurement of residual stress in TiN is considered to be reasonable for estimating the residual stress state in Al.

In the EM technique, under stressing the current above threshold current I_{th},[23] above which a wire can be grown, the average growth rate v_g of a metallic micro/nanowire is given by[23,25,26]

$$v_g = \frac{D_0}{kT}\frac{|Z^*|e\rho}{A}\exp\left(-\frac{Q-\Omega\sigma}{kT}\right)(I^* - I_{\mathrm{th}}), \tag{2}$$

where D_0 is the prefactor (m^2/s), k is the Boltzmann constant (J/K), and T is the absolute temperature (K) (the temperature increase due to Joule heating by the current stress is approximately 10 K;[24] hence, T in the Al interconnect can be assumed to be substrate temperature T_s), Z^* (<0 for Al) is the dimensionless effective charge number for EM, e is the charge of an electron (C), ρ is the electrical resistivity of an interconnect (Ω·m), A is the cross-sectional area in an interconnect (m^2), Q is the activation energy without the stress effect (J), Ω is the atomic volume (m^3/atom), σ is the hydrostatic stress in an interconnect (Pa) (note that the hydrostatic stress is represented as stress, for short, hereafter), and I^* is the net current flowing in an interconnect (A). Considering the current leakage[23] in the TiN passivation, which is correlated with the input current I_0 applied from a current source in A, I^* is proportional to I_0.[23] Previous studies[23,25] have reported the existence of I_{th} and the details regarding I^* and I_{th}. Evaluations of v_g and I_{th} contribute to the estimation of the performance of wire growth[23,25] and control of the wire shape.[24]

Figure 4(a) shows the experimental result, showing v_g as a function of I_0 for $H_{TiN} = 2.6$ (sample I) and 3.5 μm (sample II) with $D = 1.5$ and 2.0 μm. Examples of Al microwires grown by using sample I with $H_{TiN} = 2.6$ μm are shown in Figs. 4(b)–4(f). These shapes of wires follow the results reported in a previous study:[24] a higher growth rate or a smaller wire diameter favors wire straightness. It is noted that this previous study did not treat a wire with a length of less than 25 μm to distinguish whether it grows straight or not. The growth rate gradient $\partial v_g/\partial I_0$ corresponds to the slope of the approximate straight line, where v_g is proportional to I_0 based on Eq. (2): I^* is assumed to be proportional to I_0, as described above. I_{th} can be obtained at $v_g = 0$. For samples I and II with different H_{TiN}, $\partial v_g/\partial I_0$ and I_{th} clearly vary. A similar trend of $\partial v_g/\partial I_0$ was obtained from each D at sample with certain H_{TiN}: D affects the intercept of the approximate straight line as in the previous report.[25] The obtained values of $\partial v_g/\partial I_0$ and I_{th} from Fig. 4 are shown in Table I. In addition, the measurement values of

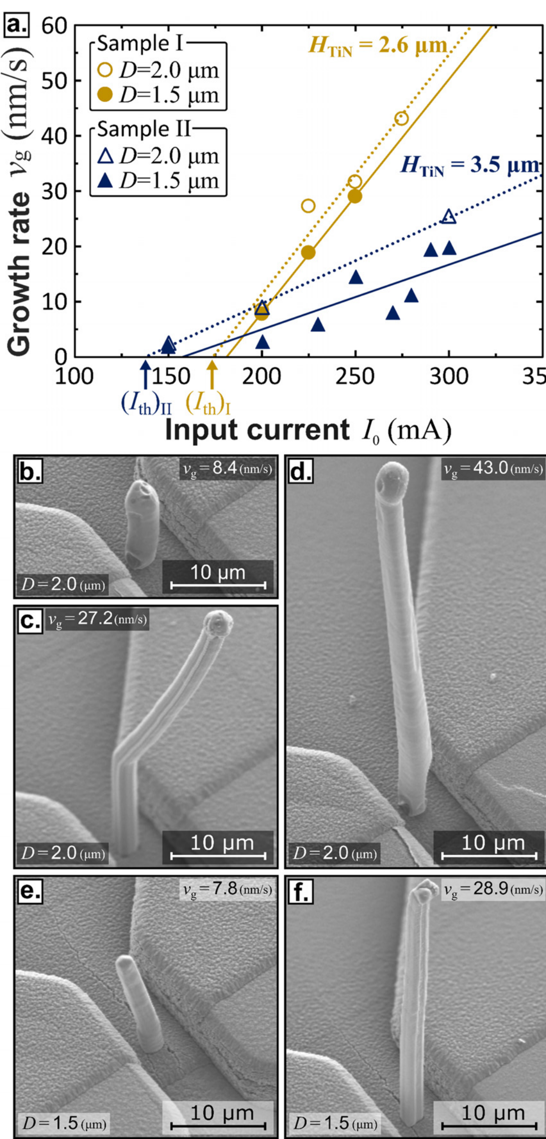

FIG. 4. (a) Graph of v_g as a function of the input current I_0, representing that thinner passivation results in greater $\partial v_g/\partial I_0$ and I_{th}. Experimental data for each H_{TiN} were obtained on the same substrate: the sample with certain H_{TiN} has many structures for the wire growth on a substrate. FE-SEM images of examples of Al microwires with (b)–(d) $v_g = 8.4$, 27.2, and 43.0 nm/s for $D = 2.0\,\mu$m and (e) and (f) $v_g = 7.8$ and 28.9 nm/s for $D = 1.5\,\mu$m, respectively, in the case of $H_{TiN} = 2.6\,\mu$m (sample I).

residual stress of TiN in samples I and II with different H_{TiN} are shown in Table I. In general, the increase in the thickness of a film deposited by sputtering increases the absolute value of the compressive residual stress in that film.[27] The obtained results in Table I represent the same trend, in which an increase in H_{TiN} increases the absolute value of the compressive residual stress of TiN. These changes in $\partial v_g/\partial I_0$ and I_{th} are presumed to be caused by the change in the residual stress in the Al interconnect, which is governed by the residual stress in TiN passivation due to H_{TiN}. In this work, only two samples with different H_{TiN} were treated. The comparison between samples with the same passivation thickness showing different residual stresses is desirable to reveal the influence of residual stress on the growth behavior of a wire. However, it is too difficult to make samples, which satisfy the above conditions. Nonetheless, Fig. 4 reflects a similar trend regarding $\partial v_g/\partial I_0$ between each D for a sample with certain H_{TiN}, and thus the experimentally obtained data can exemplify the repeatability of different H_{TiN}.

The residual stress in the Al interconnect governed by the residual stress in the overcoat TiN is speculated to influence the EM-induced localized stress due to the accumulation of atoms, expressed as σ in Eq. (2), and varies the Al atomic migration and wire growth behaviors. In fact, Lee *et al.*[28] reported that atomic migration was suppressed at a relatively high compressive stress region. To clarify the correlation between residual stress and atomic migration behavior, resulting in the growth behavior of a wire, we focus on the activation energy as a candidate for mediating the relationship between the residual stress and the growth behavior. Considering that the residual stress varies the activation energy governing atomic diffusion and growth behavior, σ in the activation energy term $Q - \Omega\sigma$ must vary with the residual stress state. In other words, the residual stress state should affect the values of $\partial v_g/\partial I_0$ and I_{th}, showing wire growth behavior through the change in activation energy term $Q - \Omega\sigma$.

To elucidate the influence of the residual stress affecting σ on the wire growth behavior representing $\partial v_g/\partial I_0$, we obtain the equation regarding σ by $\partial v_g/\partial I_0$. We obtain $\partial v_g/\partial I_0$ based on Eq. (2) as follows:

$$\frac{\partial v_g}{\partial I_0} = \frac{D_0}{kT}\frac{|Z^*|e\rho}{A}\exp\left(-\frac{Q - \Omega\sigma}{kT}\right). \tag{3}$$

The ratio of $\partial v_g/\partial I_0$ of samples I and II is given by

$$\frac{(\partial v_g/\partial I_0)_{I}}{(\partial v_g/\partial I_0)_{II}} = \exp\left[\frac{(\sigma_I - \sigma_{II})\Omega}{kT}\right], \tag{4}$$

where D_0, Z^*, ρ, A, and Q are the same between samples I and II because of the use of the same material. Therefore, the difference in σ of samples I and II, $\sigma_I - \sigma_{II}$, is expressed as

$$\sigma_I - \sigma_{II} = \frac{kT}{\Omega}\left[\ln\left(\frac{\partial v_g}{\partial I_0}\right)_I - \ln\left(\frac{\partial v_g}{\partial I_0}\right)_{II}\right]. \tag{5}$$

Equation (5) implies that the EM-induced localized stress σ can be calculated by using the experimental values of $\partial v_g/\partial I_0$. We compare with the values of $\sigma_I - \sigma_{II}$, which are experimentally measured by XRD and calculated by $\partial v_g/\partial I_0$, obtained from Fig. 4 and Eq. (5). The measured and calculated values of $\sigma_I - \sigma_{II}$ are approximately 700 and 659 MPa, respectively. The following values were used for the calculation: $k = 1.38 \times 10^{-23}$ J/K, $T = 773$ K, and $\Omega = 1.66 \times 10^{-11}\ \mu m^3$. The measured $\sigma_I - \sigma_{II}$ of 700 MPa denotes the value for the TiN passivation (but not for the Al interconnect); however, the difference in residual stress in the Al interconnect between samples I and II is considered to be equivalent to that of the TiN passivation based on Eq. (1). Because the measured and calculated values of $\sigma_I - \sigma_{II}$ are close, the residual stress state affects $\partial v_g/\partial I_0$ through σ. As a result, the increase in H_{TiN} decreases both $\partial v_g/\partial I_0$ and I_{th}. Because a larger $\partial v_g/\partial I_0$ and lower I_{th} are effective for wire growth, a conflicting effect of passivation thickness exists. In terms of $\partial v_g/\partial I_0$, an increase in the

Published under license by AIP Publishing

TABLE I. Experimental conditions and results of samples I and II.

Sample	TiN passivation thickness H_{TiN} (μm)	Hole side length D (μm)	Growth rate gradient $\partial v_g/\partial I_0$ [nm/(s·mA)]	Threshold input current I_{th} (mA)	Approximate value of residual stress in TiN measured by XRD (MPa)
I	2.6	1.5	42.2×10^{-2}	181	−600
		2.0	43.2×10^{-2}	174	
II	3.5	1.5	11.7×10^{-2}	157	−1300
		2.0	15.5×10^{-2}	137	

absolute value of the compressive residual stress with H_{TiN} influences the wire growth negatively because of an increase in the activation energy for atomic migration, which decreases $\partial v_g/\partial I_0$. Contrarily, it facilitates the initiation of wire growth because of an increase in the initial stress in the Al interconnect, decreasing I_{th}.

In conclusion, the influence of residual stress on the micro/nanowire growth behavior in the EM technique was elucidated through a comparison between the values of EM-induced localized stresses experimentally measured by XRD and calculated by the growth rate gradient obtained in the experiments. The lower absolute value of the compressive residual stress by decreasing the passivation thickness increases the growth rate owing to a lower activation energy governing atomic migration and wire growth behavior and can decrease the delamination risk of the topmost passivation, deposited by sputtering. On the other hand, a passivation that is too thin results in a lower absolute value of compressive stress, increasing the risk of passivation crack due to the accumulation of atoms by EM and increasing the threshold current. The appropriate passivation thickness should be used based on this finding.

The author gratefully acknowledges Professor Masumi Saka and Professor Hironori Tohmyoh at Tohoku University for valuable discussions. This study was supported by the JSPS KAKENHI Grant-in-Aid for JSPS Research Fellow No. 15J02134 and Early-Career Scientists No. 18K13653. This study was performed at the Micro/Nano-Machining Research and Education Center of Tohoku University.

REFERENCES

[1] I. A. Blech, J. Appl. Phys. **47**, 1203 (1976).
[2] I. A. Blech and C. Herring, Appl. Phys. Lett. **29**, 131 (1976).
[3] M. A. Korhonen, P. Børgesen, K. N. Tu, and C.-Y. Li, J. Appl. Phys. **73**, 3790 (1993).
[4] A. Mansourian, S. A. Paknejad, Q. Wen, G. Vizcay-Barrena, R. A. Fleck, A. V. Zayats, and S. H. Mannan, Sci. Rep. **6**, 22272 (2016).
[5] D. R. Strachan, D. E. Smith, D. E. Johnston, T.-H. Park, M. J. Therien, D. A. Bonnell, and A. T. Johnson, Appl. Phys. Lett. **86**, 043109 (2005).
[6] D. E. Johnston, D. R. Strachan, and A. T. C. Johnson, Nano Lett. **7**, 2774 (2007).
[7] L. Arzubiaga, F. Golmar, R. Llopis, F. Casanova, and L. E. Hueso, Appl. Phys. Lett. **102**, 193103 (2013).
[8] A. Chatterjee, T. Heidenblut, F. Edler, E. Olsen, J. P. Stöckmann, C. Tegenkamp, and H. Pfnür, Appl. Phys. Lett. **113**, 013106 (2018).
[9] I. A. Blech, P. M. Petroff, K. L. Tai, and V. Kumar, J. Cryst. Growth **32**, 161 (1976).
[10] K. Hinode, Y. Homma, and Y. Sasaki, J. Vac. Sci. Technol., A **14**, 2570 (1996).
[11] J. W. Lee, M. G. Kang, B.-S. Kim, B. H. Hong, D. Whang, and S. W. Hwang, Scr. Mater. **63**, 1009 (2010).
[12] M. Chen, Y. Yue, and Y. Ju, J. Appl. Phys. **111**, 104305 (2012).
[13] F. Ye, M. J. Burns, and M. J. Naughton, Phys. Status Solidi A **212**, 566 (2015).
[14] H.-T. Lee, Y. Kimura, and M. Saka, AIMS Mater. Sci. **5**, 591 (2018).
[15] M. W. Knight, L. Liu, Y. Wang, L. Brown, S. Mukherjee, N. S. King, H. O. Everitt, P. Nordlander, and N. J. Halas, Nano Lett. **12**, 6000 (2012).
[16] H. Honma, K. Takahashi, M. Fukuhara, M. Ishida, and K. Sawada, Micro Nano Lett. **9**, 891 (2014).
[17] J. Martin and J. Plain, J. Phys. D **48**, 184002 (2015).
[18] N. T. Nesbitt, J. M. Merlo, A. H. Rose, Y. M. Calm, K. Kempa, M. J. Burns, and M. J. Naughton, Nano Lett. **15**, 7294 (2015).
[19] F. Bisio, G. Gonella, G. Maidecchi, R. Buzio, A. Gerbi, R. Moroni, A. Giglia, and M. Canepa, J. Phys. D **48**, 184003 (2015).
[20] B.-T. Chou, Y.-H. Chou, Y.-M. Wu, Y.-C. Chung, W.-J. Hsueh, S.-W. Lin, T.-C. Lu, T.-R. Lin, and S.-D. Lin, Sci. Rep. **6**, 19887 (2016).
[21] M. Saka and R. Nakanishi, Mater. Lett. **60**, 2129 (2006).
[22] Y. Lu, H. Tohmyoh, and M. Saka, J. Phys. D **44**, 045501 (2011).
[23] Y. Kimura and M. Saka, Jpn. J. Appl. Phys., Part 1 **55**, 06GH01 (2016).
[24] Y. Kimura, Acta Mater. **157**, 276 (2018).
[25] Y. Kimura, Mech. Eng. J. **6**, 18-00269 (2019).
[26] Y. Kimura and M. Saka, in Proceedings of the 2018 Materials and Mechanics Conference of JSME GS0304 (2018) (in Japanese).
[27] X. Yan, M. Kato, and K. Nakasa, J. Soc. Mater. Sci. Jpn. **50**, 1335 (2001) (in Japanese).
[28] K.-W. Lee, H. J. Shin, Y. J. Wee, T. K. Kim, A. T. Kim, J. H. Kim, S. M. Choi, B. S. Suh, S. J. Lee, K.-K. Park, S. J. Lee, J. W. Hwang, S. W. Nam, Y. J. Moon, J. E. Ku, H. J. Lee, M. Y. Kim, I. H. Oh, J. Y. Maeng, I. R. Kim, J. E. Lee, S. M. Lee, W.-H. Choi, S. J. Park, N. I. Lee, H.-K. Kang, and G. P. Suh, in Proceedings of IEEE International Electron Devices Meeting (2004), p. 957.

Published under license by AIP Publishing